Dramatic evolution of magnetic properties induced by electronic change in $Ce(Pd_{1-x}Ag_x)_2Al_3$

2006 J. Phys.: Condens. Matter 18 5715

(http://iopscience.iop.org/0953-8984/18/24/012)

INSTITUTE OF PHYSICS PUBLISHING JOURNAL OF PHYSICS: CONDENSED MATTER

J. Phys.: Condens. Matter **18** (2006) 5715–5723 doi:10.1088/0953-8984/18/24/012

Dramatic evolution of magnetic properties induced by electronic change in $Ce(Pd_{1-x}Ag_x)_2Al_3$

Peijie Sun[1,3], Qingfeng Lu[2], Tsuyoshi Ikeno[1], Tomohiko Kuwai[1], Toshio Mizushima[1] and Yosikazu Isikawa[1]

[1] Department of Physics, Toyama University, Toyama 930-8555, Japan
[2] College of Physics and Information Engineering, Henan Normal University, Xinxinag 453007, People's Republic of China

E-mail: psun@iwate-u.ac.jp

Received 10 March 2006
Published 2 June 2006
Online at stacks.iop.org/JPhysCM/18/5715

Abstract

By measuring the lattice parameters (a, c), the magnetic susceptibility $\chi(T)$ and magnetization $M(H)$, the specific heat $C(T)$, and the electrical resistivity $\rho(T)$ for $Ce(Pd_{1-x}Ag_x)_2Al_3$, we found that with increasing x the system undergoes a variation from antiferromagnetism to ferromagnetism at $x \sim 0.05$ then back to antiferromagnetism at $x \sim 0.45$. The magnetic evolution, together with the Kondo temperature T_K that is inferred to decline with x, closely resembles that of $Ce(Pd_{1-x}Cu_x)_2Al_3$. The two systems have the same electronic but opposite volume change; resemblance between them indicates the dominant effect in the substitution is caused by electronic change but not volume change. Modification of the RKKY interaction may not account for the unusual magnetic evolution.

1. Introduction

In recent years, investigations on strongly correlated electronic systems by means of adjusting control parameters such as pressure (chemical or hydrostatic) and magnetic field have been vivid and fruitful. Quantum criticality with suppressed phase transition at 0 K represents one of the most interesting topics in this area. Chemical pressure as a convenient control parameter is frequently used to modify the hybridization between conduction and 4f(5f) localized electrons, and also the Kondo effect, the RKKY (Ruderman–Kittel–Kasuya–Yosida) interaction and the competition between them. A lot of systems illustrating this aspect have been reported, e.g., $(La_{1-x}Ce_x)_3Al$ [1], $Ce(Pd_{1-x}Ni_x)_2Al_3$ [2], and $CeRh_{1-x}Ir_xIn_5$ [3], where magnetic–nonmagnetic or magnetic–superconductivity variation is driven by chemical pressure. On the other hand, chemical replacement involving electronic change usually turns out to be complex, because electronic change may sensitively affect the band details, crystal electric

[3] Present address: Graduate School of Engineering, Iwate University, Morioka 020-8551, Japan.

field (CEF), and so on. Examples of such work are $Ce(Rh_{1-x}Ru_x)Si_2$ [4], $CeNi_{1-x}Cu_x$ [5], $Ce(Pd_{1-x}Cu_x)_2Si_2$ [6] and $CeA_{1-x}B_x$ (A, B = Zn, Ag, and Cd) [7].

$CePd_2Al_3$ is an antiferromagnetic Kondo compound with $T_N = 2.8$ K and an electronic specific heat coefficient $\gamma = 380$ mJ K^{-2} mol^{-1} [8]. The ground state is a $|\pm 1/2\rangle$ doublet. It crystallizes in the $PrNi_2Al_3$-type hexagonal structure, in which the basal planes consisting of Ce and Pd atoms alternate with the Al layers along the c-axis. Recently, we found that introducing Cu into the Pd site in $CePd_2Al_3$ drives the magnetic ground state from antiferromagnetism to ferromagnetism then back to antiferromagnetism (AFM–FM–AFM) according to the Cu concentration [9]. There, electronic change induced by the extra d electron of Cu with respect to Pd is supposed to be responsible for the magnetic evolution.

In this work we use Ag, instead of Cu, to replace Pd in $CePd_2Al_3$. This investigation is very worthwhile because Cu and Ag induce opposite volume change as well as the same electronic change. The lattice parameters (a, c), the magnetic susceptibility $\chi(T)$, the magnetization $M(H)$, the electrical resistivity $\rho(T)$, and the specific heat $C(T)$ were measured for $Ce(Pd_{1-x}Ag_x)_2Al_3$. A striking resemblance in magnetic evolution between Ag and Cu replacements is observed in spite of the opposite lattice change. This point is of interest because an opposite lattice change is normally expected to modify the Kondo effect and RKKY oppositely. We will show that the electronic change induced by Ag overwhelms the change in lattice dimensions in this system, and the modification of the RKKY interaction cannot account for the magnetic evolution.

2. Experimental details

Polycrystalline samples of $Ce(Pd_{1-x}Ag_x)_2Al_3$ were synthesized by arc-melting stoichiometric amounts of Ce, Pd, Ag, Al with purity 99.9%, 99.95%, 99.999% and 99.999%, respectively. An annealing treatment was performed in evacuated quartz tubes for 100–150 h at 900 °C, in the same way as for $Ce(Pd_{1-x}Cu_x)_2Al_3$ [9]. Such a heat treatment has been reported to be very effective to establish a well-defined magnetic ordering in $CePd_2Al_3$ [8, 10]. Several samples of $La(Pd_{1-x}Ag_x)_2Al_3$ were also synthesized, as the corresponding non-magnetic compounds for estimating the magnetic contribution in the Ce samples.

X-ray diffraction on powdered samples was carried out for all the prepared samples to evaluate the crystal structure and to determine the lattice parameters. The electrical resistivity ρ was measured using a standard four-probe DC method in the temperature range from 1.8 K to room temperature. The magnetic susceptibility χ and magnetization M measurements were performed with a superconducting quantum interference device (SQUID) magnetometer (Quantum Design Co., Ltd). It should be noted that powdered samples were used in the magnetic measurements because preferred crystallographic orientation is confirmed in the bulk ones. The specific heat C was measured with an adiabatic (or quasi-adiabatic) method from 1.6 to 30 K, while for compositions of interest ($x = 0.05$, 0.4, 0.45 and 0.5) down to ~0.5 K an Oxford dilution refrigerator or a ^{3}He refrigerator was used.

3. Results and discussions

The x-ray powder diffraction patterns for $Ce(Pd_{1-x}Ag_x)_2Al_3$ show that the single $PrNi_2Al_3$-type hexagonal phase extends to $x = 0.6$, and a second phase of $BaAl_4$-type tetragonal structure begins to emerge gradually for higher x. We therefore limit our research to $x \leqslant 0.6$ in this work. The x-dependent lattice parameters a and c, unit-cell volume v, and the ratio c/a of $Ce(Pd_{1-x}Ag_x)_2Al_3$ are shown in figure 1. Obviously, a, c and v expand with x obeying Vegard's law. For the concentration $x = 0.6$, the unit-cell volume expands by a factor of 3.1%

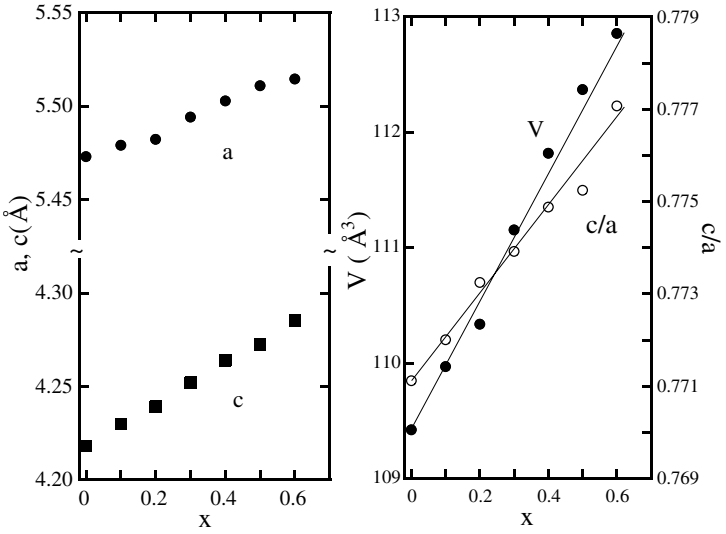

Figure 1. Lattice parameters a and c, unit-cell volume v, and the ratio c/a of $Ce(Pd_{1-x}Ag_x)_2Al_3$.

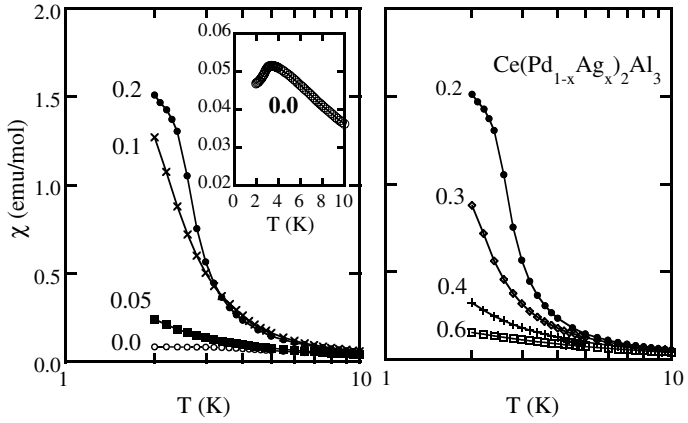

Figure 2. Magnetic susceptibility χ measured at H = 1 kOe as a function of $\log T$ for $Ce(Pd_{1-x}Ag_x)_2Al_3$. Note the enhancing process of χ with x in the left panel and the weakening process in the right panel.

compared to $x = 0.0$. The lattice parameter c expands faster than a, so the ratio c/a increases with x, from 0.771 ($x = 0$) to 0.777 ($x = 0.6$) almost linearly. The variation of a, c, v, together with c/a, are all counter to those of $Ce(Pd_{1-x}Cu_x)_2Al_3$ [9]. This degree of lattice expansion is considerable and comparable to that of other systems, like $CeRh_{1-x}Ir_xIn_5$, where evolution between magnetism and superconductivity is driven by substitution [3]. The lattice of $La(Pd_{1-x}Ag_x)_2Al_3$ changes (not shown here) as a function of x in the same way as the Ce counterpart.

Shown in figure 2 is the magnetic susceptibility χ versus $\log T$ in the temperature range 2 K $< T <$ 10 K. The applied external magnetic field is $H = 1$ kOe in the measurements. These curves resemble those of $Ce(Pd_{1-x}Cu_x)_2Al_3$, where ferromagnetic ordering appears by

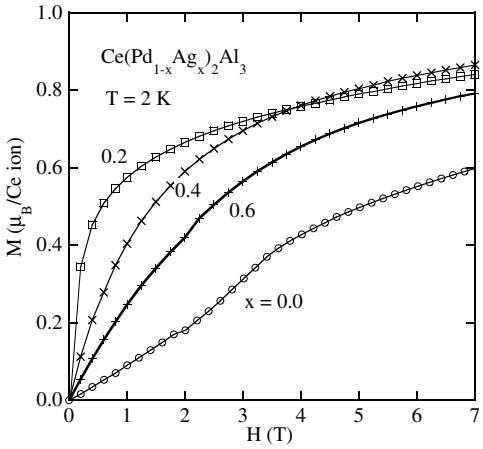

Figure 3. Magnetization curves of $Ce(Pd_{1-x}Ag_x)_2Al_3$ for $x = 0.0$, 0.2, 0.4 and 0.6.

introducing 10–40% Cu [9]. For $x = 0.0$, a clear peak indicating the antiferromagnetic ordering is observed (inset of figure 2). With increasing x, χ at low temperatures is enhanced by an order of magnitude. For $x = 0.2$, an apparent saturating trend with enhanced values is observed at $T < 3$ K, characteristic of ferromagnetism. For larger x exceeding 0.2, χ decreases again. For $x = 0.6$, χ has small values comparable with those at $x = 0.0$. χ at $T > 100$ K conforms to the Curie–Weiss behaviour for all the samples and gives an effective magnetic moment μ_{eff} close to that of a free Ce^{3+} ion. However, the paramagnetic Curie temperatures θ_P estimated from the same temperature range are all negative, indicating that the interaction is antiferromagnetic at high temperatures for all the samples.

$M(H)$ curves at 2 K for representative x are shown in figure 3. A rapid rise of M at low magnetic fields characteristic of ferromagnetic interaction is observed for $x = 0.2$, whereas for $x = 0.0$ and 0.6, metamagnetic behaviour characteristic of antiferromagnetic ordering is observable at around 3 and 2 T, respectively. M values for $x = 0.6$ are much larger compared to those for $x = 0.0$ although both of them are antiferromagnetic. This can be understood if one considers the evolution of the Kondo effect discussed later.

In figure 4, we show the magnetic contribution to the specific heat, C_{mag}, for $Ce(Pd_{1-x}Ag_x)_2Al_3$ below 6 K. C_{mag} is estimated by subtracting C of the La counterpart from that of the Ce one as described elsewhere [12]. Coinciding with the x dependence of $\chi(T)$ and $M(H)$ curves, a similarity to $Ce(Pd_{1-x}Cu_x)_2Al_3$ is also found in C_{mag}. The peak of the magnetic transition at 2.8 K for $x = 0.0$ shifts rapidly to lower temperature on increasing x to 0.02 and 0.05. It is small and somewhat obscure for $x = 0.05$. On increasing x to 0.1 and 0.2, it shifts to higher temperature again, with enhanced values. For $x = 0.2$, the peak is at 2.4 K and is of λ-type. On increasing x further from 0.2 to 0.6, one more cycle of the peak's variation as described above takes place, with $x \sim 0.45$ being the crossover. Around the crossover, the $C_{\text{mag}}(T)$ curve changes little when increasing $x = 0.4$ to 0.45 and to 0.5, indicating the complexity of the magnetism. All the peak temperatures are given in table 1.

Analogous to the magnetic evolution of $Ce(Pd_{1-x}Cu_x)_2Al_3$, a similar magnetic phase diagram of T_N (or T_C) versus x is constructed for $Ce(Pd_{1-x}Ag_x)_2Al_3$ (figure 5). The antiferromagnetic state disappears rapidly with a slight replacement of less than 10% of Ag, followed by a ferromagnetic state for $0.1 < x < 0.4$; then the antiferromagnetic ground state appears again after increasing x over 0.5. This phase diagram closely resembles that of the Cu

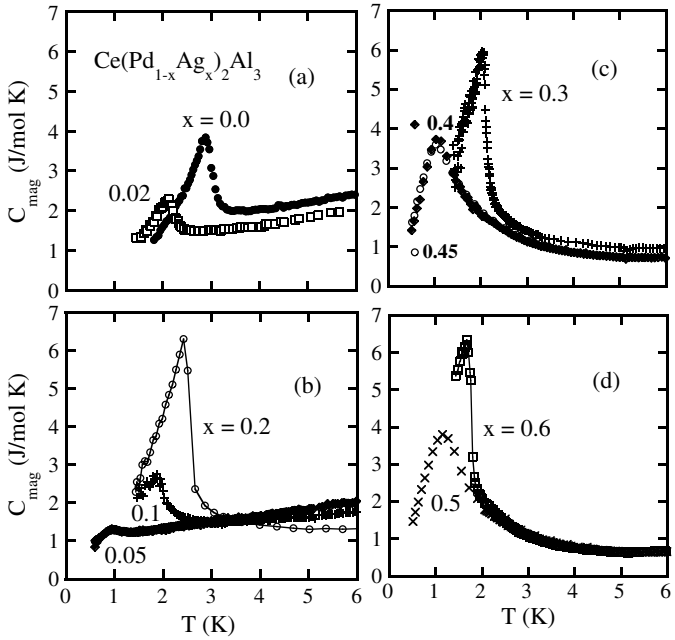

Figure 4. Magnetic contribution to the specific heat, $C_{\rm mag}$, as a function of temperature for $Ce(Pd_{1-x}Ag_x)_2Al_3$. The curves are arranged in four panels for a clearer understanding of the systematic variation of the peak temperature and the height.

Table 1. The magnetic ordering temperature $T_{\rm N}$ (or $T_{\rm C}$), the electrical resistivity at $T = 280$ K, $\rho_{280\ {\rm K}}$, the magnetic entropy evolved by the ordering temperature, $S_{\rm order}$, and the calculated Kondo temperature $T_{\rm K}$ for $Ce(Pd_{1-x}Ag_x)_2Al_3$.

x	$T_{\rm N}$, $T_{\rm C}$ (K)	$\rho_{280\ {\rm K}}$ ($\mu\Omega$ cm)	$S_{\rm order}$ ($R\ln 2$)	$T_{\rm K}$ (K)
0.0	2.8	168.6	0.29	8.2
0.02	2.1	—	0.29	6.1
0.05	1.0	83.5	0.28	3.0
0.1	1.9	96.0	0.50	4.0
0.2	2.4	104.6	0.66	3.8
0.3	2.0	47.8	0.61	3.5
0.4	1.0	53.2	0.49	2.1
0.45	1.0	—	0.49	2.1
0.5	1.1	52.6	0.57	2.1
0.6	1.7	38.9	0.80	1.9

substitution system. The magnetic properties around the two crossovers, i.e., $x \sim 0.05$ and 0.45 seem complex and are not clear at the moment. Spin glass may be possible in the crossovers due to the competition between antiferromagnetic and ferromagnetic interactions among the magnetic ions [11].

Shown in figure 6(a) is the magnetic entropy $S_{\rm mag}$ as a function of T below 15 K. $S_{\rm mag}(T)$ is obtained by numerical integration of $C_{\rm mag}/T$ with respect to T, with its initial value at the lowest experimental temperature estimated by means of extrapolation. Here we limit the discussion to this low-temperature range to avoid the influence of the CEF that is observed to change with x [12]. $S_{\rm mag}$ is enhanced by Ag substitution, amounting to 80% of $R\ln 2$ (the

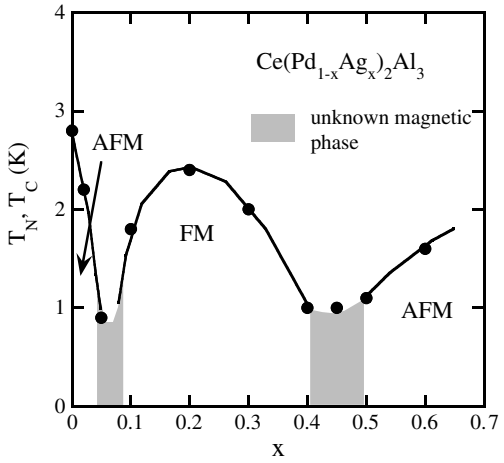

Figure 5. Temperature–composition phase diagram of $Ce(Pd_{1-x}Ag_x)_2Al_3$. The ordering temperatures are taken from the peak in specific heat.

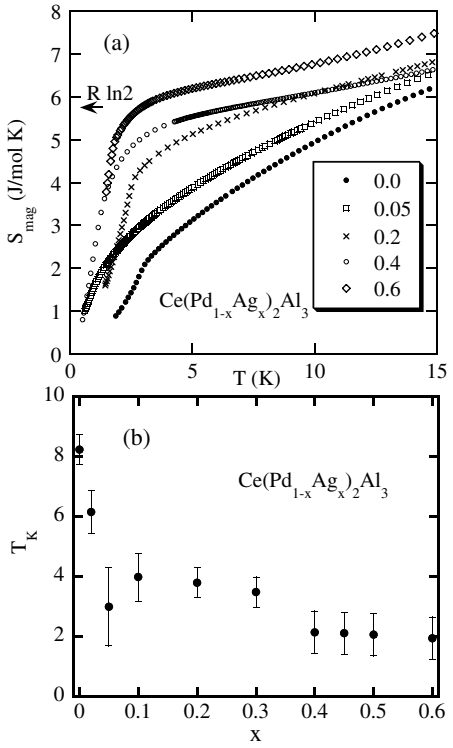

Figure 6. (a) Magnetic entropy S_{mag} as a function of temperature. (b) Kondo temperature T_k as a function of Ag concentration x.

whole entropy of the magnetic ground doublet) by the ordering temperature for $x = 0.6$. The Kondo temperature T_K is estimated using the formularized relation between the magnetic

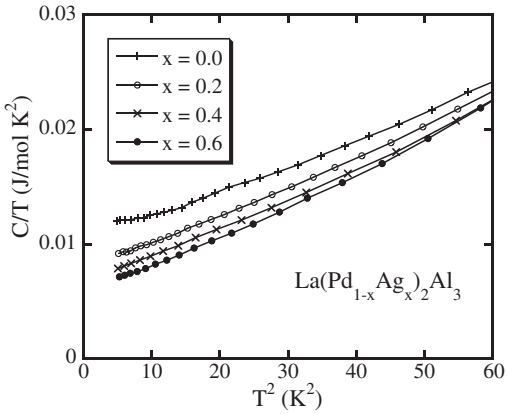

Figure 7. Specific heat of $La(Pd_{1-x}Ag_x)_2Al_3$ for $x = 0.0, 0.2, 0.4, 0.6$ plotted as C/T versus T^2.

Table 2. Electrical specific heat coefficient γ and Debye temperature θ_D obtained by fitting the C/T versus T^2 curve to $C = \gamma T + \beta T^3$ for $La(Pd_{1-x}Ag_x)_2Al_3$.

Compound	γ (mJ mol^{-1} K^{-2})	θ_D (K)
$LaPd_2Al_3$	9.7	369
$La(Pd_{0.8}Ag_{0.2})_2Al_3$	7.7	364
$La(Pd_{0.6}Ag_{0.4})_2Al_3$	6.5	362
$La(Pd_{0.4}Ag_{0.6})_2Al_3$	5.6	357

entropy evolved by ordering temperature, S_{order}, and the ratio $Q = T_K/T_{order}$ as follows [13].

$$\frac{S_{order}}{R} = \ln[1 + \exp(-Q)] + Q\left[\frac{\exp(-Q)}{1 + \exp(-Q)}\right].$$

The S_{order} s and the calculated T_K s are listed in table 1. T_K as a function of x, shown in figure 6(b), is substantially the same as that of $Ce(Pd_{1-x}Cu_x)_2Al_3$, decreasing roughly with increasing x in spite of the opposite lattice change. Unlike the Cu substitution, the negative volume effect of Ag substitution itself may induce a decrease of T_K; however, the extreme resemblance between the two systems distinctly indicates that the variation of T_K arises from electronic change.

The specific heat of the La compounds is useful for understanding the T_K evolution in Ce compounds, and is shown in figure 7. Here a contributing factor to T_K will be discussed, namely the density of states in the conduction band at the Fermi level, $N(E_F)$. Linear fits to the C/T versus T^2 curves in figure 7 are excellent for all the concentrations (for $x = 0.0$, small impurities are also observed). The obtained electronic specific heat coefficient γ and Debye temperature θ_D decrease with x (table 2). These results mean $N(E_F)$ decreases with increasing x, in contrast to the progressive increase of the conduction electron density. The same fact is also found in other electronic change systems, e.g., $Ce(Pd_{1-x}Cu_x)_2Si_2$ [6], where with increasing Cu concentration, the d band is found to be filled and consequently lowered far below the Fermi energy, leading to a decrease of $N(E_F)$. Following the relation $T_K \sim \exp[-1/(J_{cf}N(E_F)]$, one knows that T_K will decrease with $N(E_F)$. For a detailed analysis, the variation of J_{cf} as a function of x should be taken into account too. Theoretically, Monachesi *et al* investigated the hybridization between conduction and f electrons as a function of composition for $CeCd_{1-x}Ag_x$, $CeCd_{1-x}Zn_x$ and $CeAg_{1-x}Zn_x$ [7]. They concluded that the

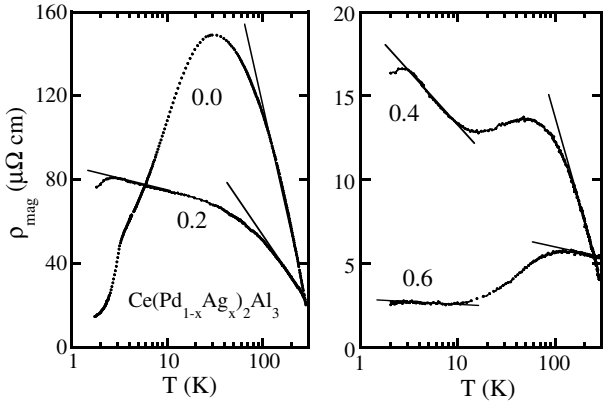

Figure 8. Magnetic contribution to electrical resistivity, $\rho_{\rm mag}$, versus $\log T$ of $Ce(Pd_{1-x}Ag_x)_2Al_3$ for $x = 0.0$, 0.2, 0.4 and 0.6. Note the different scales of the vertical axes of the two panels.

volume effect plays a minor role compared to the electronic effect in alloyed systems. This is also the case with the present system.

The electrical resistivity ρ of this system also presents evidence for the evolution of Kondo scattering. Figure 8 shows the magnetic contribution $\rho_{\rm mag}$ as a function of $\log T$, which is estimated by subtracting the corresponding ρ of the La counterpart. The gradual reduction of $\rho_{\rm mag}$ with x over the whole temperature range is consistent with the inference that the Kondo effect weakens. Typical condensed Kondo behaviour with a coherence effect at $T < 30$ K is observed for $x = 0$, for which linear $-\ln T$ dependence characterizing Kondo scattering is observed at high temperatures. For the other three samples, two separated linear $-\ln T$ regions are observed, indicating the CEF energy splitting. One more significant point in figure 8 is the deduction of both the high-T and low-T slopes of the logarithmic part. The slope at temperatures much lower or higher than a certain CEF splitting energy has been theoretically calculated by Cornut and Coqblin [14], and is shown to reflect the product $J_{\rm cf}^3 N(E_{\rm F})^2$. Consequently, the decline of the slopes is also consistent with the decrease of the Kondo temperature $T_{\rm K}$.

We turn again to consider the close resemblance of magnetic evolutions seen in $Ce(Pd_{1-x}M_x)_2Al_3$ for M = Cu and Ag. We reasonably suppose that Ag and Cu substitutions for Pd give rise to the same effect on the electronic details of $Ce(Pd_{1-x}M_x)_2Al_3$; therefore, the only difference between the two systems that remains is the volume effect. If modification of the RKKY interaction accounts for the AFM–FM–AFM evolution, Cu and Ag substitutions are expected to produce different magnetic behaviours due to the opposite lattice change of the Ce–Ce and Ce–M distances, and of the c/a ratio. Therefore, modification of the RKKY interaction may not account for the magnetic evolution in the present system. Actually, the RKKY interaction has been experimentally confirmed to be very sensitive to the c/a change in a comparative study of the antiferromagnetic $CePd_2Al_3$, and the ferromagnetic $CePd_2Ga_3$ with $T_{\rm C} \simeq 6$ K [15]. Here the important points are that Al and Ga have the same electronic configuration, and the replacement of Al by Ga takes place out of Ce planes and enhances the c/a. Modification of the RKKY interaction is supposed to account for this AFM–FM variation of the Al/Ga replacement [16].

The specific heat at relatively higher temperatures up to 150 K has been shown elsewhere for $Ce(Pd_{1-x}M_x)_2Al_3$ (M = Ag or Cu) [12], where we observed an unusual Schottky peak when Ag (or Cu) is introduced, and discussed the replacement-induced randomness in the CEF

potential as a possible origin of the AFM–FM–AFM variation in this system. The electrical difference between Ag (or Cu) and Pd ions, and the chemical disorder in the substitution, will cause randomness in the CEF potential. The peculiar magnetic structure of $CePd_2Al_3$, where spins align ferromagnetically in the basal planes of the hexagonal structure and the ferromagnetic planes are stacked antiferromagnetically along the c-axis [17], may be another key point in understanding the unique magnetic evolution. A microscopic study on the magnetic structure using a single crystal is desired to clarify the magnetic evolution.

4. Conclusion

To summarize, we investigated the magnetic, thermal, and transport properties of the substitutional system $Ce(Pd_{1-x}Ag_x)_2Al_3$, in comparison to its homologous system $Ce(Pd_{1-x}Cu_x)_2Al_3$. A weakening of the Kondo temperature T_K and a complex magnetic phase diagram showing alternation between AFM and FM states were found, similar to the latter system. Through this work, the dominant role of the extra d electron provided by Ag (or Cu) in the magnetic evolution is confirmed distinctly, overwhelming the volume change effect. Modification of the RKKY interaction cannot describe the magnetic evolution. The change of T_K is at least partially caused by variation of $N(E_F)$ of the conduction band.

References

[1] Medina A N, Hayashi M A, Cardoso L P, Gama S and Gandra F G 1998 *Phys. Rev.* B **57** 5900
[2] Isikawa Y, Sakai H, Mizushima T, Kuwai T and Sakurai J 2002 *Physica* B **312/313** 259
[3] Pagliuso P G, Petrovic C, Movshovich R, Hall D, Hundley M F, Sarrao J L, Thompaon J D and Fisk Z 2001 *Phys. Rev.* B **64** 100503
[4] Lloret B, Chevalier B, Buffat B, Etourneau J, Quezel S, Lamharrar A, Rossat-Mignod J, Calemczuk R and Bonjour E 1987 *J. Magn. Magn. Mater.* **63/64** 85
[5] García Soldevilla J, Gómez Sal J C, Blanco J A, Espeso J I and Rodríguez Fernández J 2000 *Phys. Rev.* B **61** 6821
[6] Gomez Berisso M, Trovarelli O, Pedrazzini P, Zwicknagl G, Geibel C, Steglich F and Sereni J G 1998 *Phys. Rev.* B **58** 314
[7] Monachesi P and Continenza A 1993 *Phys. Rev.* B **47** 14622
[8] Kitazawa H, Schank C, Thies S, Seidel B, Geibel C and Steglich F 1992 *J. Phys. Soc. Japan* **61** 1461
[9] Sun P, Isikawa Y, Lu Q, Huo D and Kuwai T 2003 *J. Phys. Soc. Japan* **72** 916
[10] Mentink S A M, Bos N M, Nieuwenhuys G J, Menovsky A A and Mydosh J A 1993 *Physica* B **186–188** 497
[11] Mydosh J A 1996 *J. Magn. Magn. Mater.* **157/158** 606
[12] Sun P, Lu Q, Kobayashi K, Kuwai T and Isikawa Y 2004 *Phys. Rev.* B **70** 174429
[13] Yashima H, Mori H, Sato N, Satoh T and Kohn K 1983 *J. Magn. Magn. Mater.* **31–34** 411
[14] Cornut B and Coqblin B 1972 *Phys. Rev.* B **5** 4541
[15] Bauer E, Schaudy G, Hilscher G, Keller L, Fischer P and Dönni A 1994 *Z. Phys.* B **94** 359
[16] Burghardt T, Hallmann E and Eichler A 1997 *Physica* B **230–232** 214
Burghardt T, Eichler A, Süllow S and Mydosh J A 1999 *Physica* B **259–261** 99
[17] Mitsuda S, Wada T, Hosoya K, Yoshizawa H and Kitazawa H 1992 *J. Phys. Soc. Japan* **61** 4667